

広島大学学術情報リポジトリ  
Hiroshima University Institutional Repository

Title	Photodynamic Activities of Porphyrin Derivative-Cyclodextrin Complexes by Photoirradiation
Author(s)	Ikeda, Atsushi; Satake, Shuhei; Mae, Tomoya; Ueda, Masafumi; Sugikawa, Kouta; Shigeto, Hajime; Funabashi, Hisakage; Kuroda, Akio
Citation	ACS Medicinal Chemistry Letters , 8 (5) : 555 - 559
Issue Date	2017-05-11
DOI	<a href="https://doi.org/10.1021/acsmchemlett.7b00098">10.1021/acsmchemlett.7b00098</a>
Self DOI	
URL	<a href="https://ir.lib.hiroshima-u.ac.jp/00046209">https://ir.lib.hiroshima-u.ac.jp/00046209</a>
Right	Copyright (c) 2017 American Chemical Society This document is the Accepted Manuscript version of a Published Work that appeared in final form in 'ACS Medicinal Chemistry Letters', copyright © American Chemical Society after peer review and technical editing by the publisher. To access the final edited and published work see <a href="https://doi.org/10.1021/acsmchemlett.7b00098">https://doi.org/10.1021/acsmchemlett.7b00098</a> . This is not the published version. Please cite only the published version. この論文は出版社版ではありません。引用の際には出版社版をご確認ご利用ください。
Relation	



# Photodynamic Activities of Porphyrin Derivative–Cyclodextrin Complexes by Photoirradiation

Atsushi Ikeda,<sup>\*,†</sup> Shuhei Satake,<sup>†</sup> Tomoya Mae,<sup>†</sup> Masafumi Ueda,<sup>†</sup> Kouta Sugikawa,<sup>†</sup> Hajime Shigeto,<sup>‡</sup> Hisakage Funabashi,<sup>‡</sup> and Akio Kuroda<sup>‡</sup>

<sup>†</sup>Department of Applied Chemistry, Graduate School of Engineering, Hiroshima University, 1-4-1 Kagamiyama, Higashi-Hiroshima 739-8527, Japan

<sup>‡</sup>Department of Molecular Biotechnology, Graduate School of Advanced Sciences of Matter, Hiroshima University, 1-3-1 Kagamiyama, Higashi-Hiroshima, Hiroshima 739-8530, Japan

**KEYWORDS:** porphyrin, cyclodextrin, photodynamic therapy, photosensitizer

**ABSTRACT:** Water-soluble cyclodextrin (CyD)-complexed with porphyrin derivatives with different substituents in the *meso*-positions showed different photodynamic activities toward cancer cells under illumination at wavelengths over 600 nm, the most suitable wavelengths for photodynamic therapy (PDT). In particular, aniline- and phenol-substituted derivatives had high photodynamic activity because of the efficient intracellular uptake of the complexes by tumor cells. These complexes showed greater photodynamic activity than photofrin, currently the main drug in clinical use as a photosensitizer. These results represent a significant step towards the optimization of porphyrin derivatives as photosensitizers.

Porphyrins have been widely investigated as potential photosensitizers (PSs).<sup>1–3</sup> During photodynamic therapy (PDT), an intravenously administered PS is allowed to accumulate in a tumor. Selective light-irradiation is then used to produce reactive oxygen species (ROS) by photochemical reactions between photoexcited PS and molecular oxygen.<sup>4</sup> Therefore, water-solubilization of PSs is very important for biological applications such as PDT. Water-soluble porphyrins and their derivatives have been synthesized by introduction of hydrophilic moieties.<sup>1–3</sup> However, the introduction of the hydrophilic moieties frequently results in insufficiently water-soluble porphyrin derivatives due to self-aggregation of the compounds. Therefore, these porphyrin derivatives are commonly injected into cells or the body as an aqueous solution with dimethyl sulfoxide or ethanol solutions, both of which are highly cytotoxic.<sup>5–7</sup> An alternative approach is to use solubilizing agents such as water-soluble polymers,<sup>8</sup> cyclodextrins,<sup>9–11</sup> or liposomes.<sup>12</sup> The complexes of the porphyrin derivatives with cyclodextrins are especially easy to prepare with a mechanochemical high-speed-vibration milling apparatus.<sup>12–14</sup> In this paper, we compare the photodynamic activities of porphyrin derivatives with different substituents in *meso*-positions, complexed with trimethyl- $\beta$ -cyclodextrin (TMe- $\beta$ -CyD; Figure 1). Photodynamic activities were evaluated with HeLa cells through irradiation with visible-light at long wavelengths (610–740 nm), the optimal wavelengths for PDT.

Complexes of porphyrin derivatives (**1–6**) with TMe- $\beta$ -CyD (Figure 1) were formed as previously described.<sup>12–14</sup> The formation of these materials was confirmed by UV-vis absorption and <sup>1</sup>H NMR spectroscopy (Figures 2, S1, and S2). These spectra indicated that compounds **1–6** all formed

complexes with two TMe- $\beta$ -CyDs. They were all soluble in water and stable at room temperature (Figure 1).

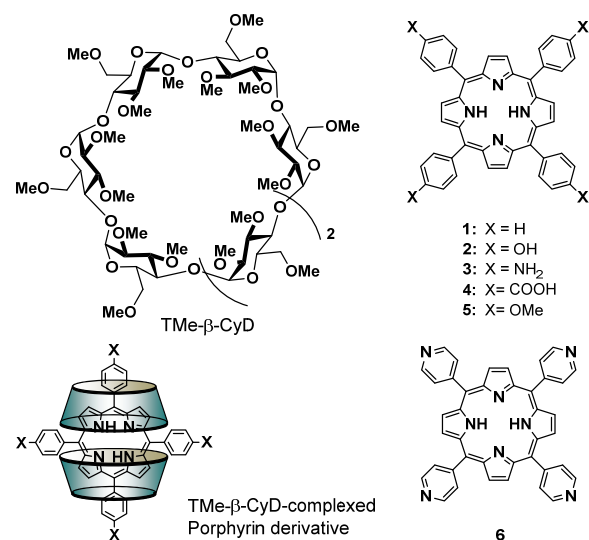


**Figure 1.** Compound structures and schematic illustration of the TMe- $\beta$ -CyD-complexed with porphyrin derivatives.

We first investigated the levels and kinds of generated cytotoxic ROS and the stability of the TMe- $\beta$ -CyD-complexed with porphyrin derivatives under visible-light irradiation at a wavelength greater than 620 nm. Photoexcited porphyrins transfer an electron to molecular oxygen (<sup>3</sup>O<sub>2</sub>) to give superoxide anions (O<sub>2</sub><sup>•-</sup>) (electron-transfer pathway Type I), and transfer energy to <sup>3</sup>O<sub>2</sub> to give singlet oxygen

molecules ( $^1\text{O}_2$ ) (energy-transfer pathway Type II).<sup>15</sup> To identify the reactive oxygen species, the presence of  $^1\text{O}_2$  and  $\text{O}_2^{\cdot-}$  was analyzed with 9,10-anthracenediyl-bis(methylene)dimalonic acid (ABDA) and nitroblue tetrazolium (NBT), respectively.<sup>15-18</sup> Conversion to an endoperoxide from ABDA by reaction with  $^1\text{O}_2$  leads to a decrease in absorbance at 380 nm (Figures S3 and S4). Generation of formazan, reduced NBT by  $\text{O}_2^{\cdot-}$ , is observed as an increase in absorption at 560 nm (Figure S5). The decrease of ABDA was plotted as a function of photoirradiation time of the complexes in aqueous solutions. The TMe- $\beta$ -CyD-complexed with **1**, **5**, and **6** precipitated out not only after vigorous bubbling of oxygen but also after photoirradiation, suggesting that these complexes were destabilized by photoactivation (Figures S3a, S4b, and S4c). As shown by their precipitation with oxygen gas bubbling and photoirradiation, these complexes are unstable due to the effect of the substituents in the *meso*-positions.<sup>10</sup> Therefore, compound **2** was employed as a neutral guest molecule in the place of **1**. The TMe- $\beta$ -CyD-complexed with **2** was stable in water after photoirradiation. Cationic **3** and anionic **4** were also stable as complexes with TMe- $\beta$ -CyD after photoirradiation. The absorption level of ABDA at 380 nm (the absorption maximum of ABDA) was plotted as a function of photoirradiation time of the TMe- $\beta$ -CyD-complexed with **2-4** (15  $\mu\text{M}$ ) in  $\text{O}_2$ -saturated aqueous solutions (Figure 3a). The results show that these TMe- $\beta$ -CyD complexes generated  $^1\text{O}_2$  in the order of  $3 > 2 \approx 4$ ; however, the differences were very small. The difference between **2** and **3** in the photoproduction abilities of  $^1\text{O}_2$  simply reflects the amount of light absorption over 620 nm (Figure 2 inset, black and red lines).<sup>17</sup> However, **4** displayed relatively high  $^1\text{O}_2$  photoproduction, despite the low absorption over 620 nm (Figure 2 inset, blue line).

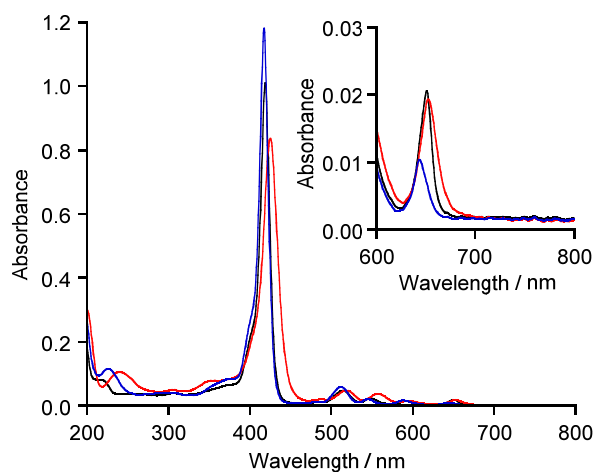


**Figure 2.** UV-vis absorption spectra of the TMe- $\beta$ -CyD-complexed with **2** (black line), the TMe- $\beta$ -CyD-complexed with **3** (red line), and TMe- $\beta$ -CyD-complexed with **4** (blue line; [TMe- $\beta$ -CyD-complexed with **2-4**] = 30  $\mu\text{M}$ ). All absorption spectra were measured in  $\text{H}_2\text{O}$  at 25  $^\circ\text{C}$  (1 mm cell).

In contrast, reduction of NBT by  $\text{O}_2^{\cdot-}$  could not be detected in the photoirradiated TMe- $\beta$ -CyD-complexed with **2-4**, even though formazan was readily detected in the positive control sample TMe- $\beta$ -CyD-complexed with **2** in the presence of NADH (Figure 3b).<sup>19</sup> These results suggest that

ROS produced by the TMe- $\beta$ -CyD-complexed with porphyrin derivatives of **2-4** are mostly  $^1\text{O}_2$ , generated by a Type II reaction.

Next the photodynamic activities of the TMe- $\beta$ -CyD-complexed with porphyrin derivatives were evaluated *in vitro* on HeLa (human cervical carcinoma) cells. The cells were

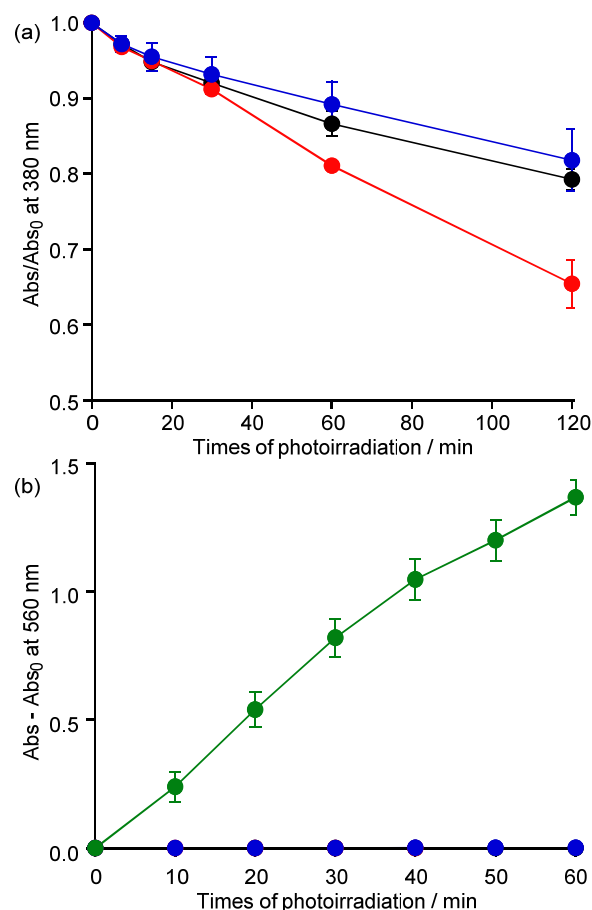


**Figure 3.** Detection of  $^1\text{O}_2$  and  $\text{O}_2^{\cdot-}$  generation by chemical methods. (a) The ABDA bleaching method was used to detect the generation of  $^1\text{O}_2$ . The bleaching of ABDA was monitored as a decrease in the absorbance at 380 nm ([TMe- $\beta$ -CyD-complexed with **2-4**] = 15  $\mu\text{M}$ , [ABDA] = 25  $\mu\text{M}$ ). (b) The NBT method was used to detect generation of  $\text{O}_2^{\cdot-}$ . The amount of formazan product, which was generated by reduction of NBT in the presence of  $\text{O}_2^{\cdot-}$ , was analyzed spectrophotometrically at an absorbance of 560 nm. TMe- $\beta$ -CyD-complexed with **2**: black line, TMe- $\beta$ -CyD-complexed with **3**: red line, TMe- $\beta$ -CyD-complexed with **4**: blue line, TMe- $\beta$ -CyD-complexed with **3** in the presence of NADH (positive control): green line. ([TMe- $\beta$ -CyD-complexed with **2-4**] = 50  $\mu\text{M}$ , [NBT] = 0.20 mM, [NADH] = 0 or 0.50 mM). All samples were photoirradiated at wavelengths  $>$  620 nm in  $\text{O}_2$ -saturated aqueous solutions. Error bars represent the mean  $\pm$  standard deviation (SD) for  $n = 3$ .

incubated with 0.02–0.4  $\mu\text{M}$  of the TMe- $\beta$ -CyD-complexed with porphyrin derivatives for 24 h before photoirradiation with wavelengths greater than 610 nm (610–740 nm) for 30 min. Photoirradiation was carried out under 9  $\text{mW cm}^{-2}$  light power at the cell level. The cell survival rate was determined using a WST-8 assay with a Cell Counting Kit-8. The

results are summarized in Figure 4. Under dark conditions, the TMe- $\beta$ -CyD-complexed with porphyrin derivatives of **2**–**4** show no cytotoxicity to the HeLa cells (Figure 4a). The TMe- $\beta$ -CyD that remained in the HeLa cells did not influence the results because the toxicities of  $\beta$ -CyD and their derivatives followed the general trend DMe- $\beta$ -CyD >>  $\beta$ -CyD > TMe- $\beta$ -CyD.<sup>20</sup> Furthermore, the TMe- $\beta$ -CyD-complexed with **4** showed no photodynamic activity. In contrast, the TMe- $\beta$ -CyD-complexed with **2** and **3** showed photodynamic activities in a dose-dependent manner, with half maximal inhibitory concentration ( $IC_{50}$ ) values of 0.15 and 0.08  $\mu$ M, respectively (Figure 4b). The TMe- $\beta$ -CyD-complexed with **4** had a very low photodynamic activity in spite of a similar structure to TMe- $\beta$ -CyD-complexed with **2**. Because the TMe- $\beta$ -CyD-complexed with **2** and **4** generate a similar amount of  $^1O_2$ , we suggest the phenol moieties of **2** play a key role in intracellular uptake of the complex by HeLa cells. Detail of this intracellular uptake is described below. In these TMe- $\beta$ -CyD complexes, the order of the photodynamic activity was **3** > **2** >> **4**. The  $IC_{50}$  values of the TMe- $\beta$ -CyD-complexed with **2** and **3** are lower than that of photofrin, presently used as the main drug in clinical photosensitizers. Here, the molar numbers of photofrin were converted to moles of porphyrin units because photofrin consists of hematoporphyrin esters and ethers containing monomers, dimers and oligomers. Figure 4b shows  $IC_{50}$  value of 2.1  $\mu$ M for photofrin under the same conditions as described above. The TMe- $\beta$ -CyD-complexed with **2** and **3** had approximately 14 and 26 times higher photodynamic activities than photofrin, respectively.

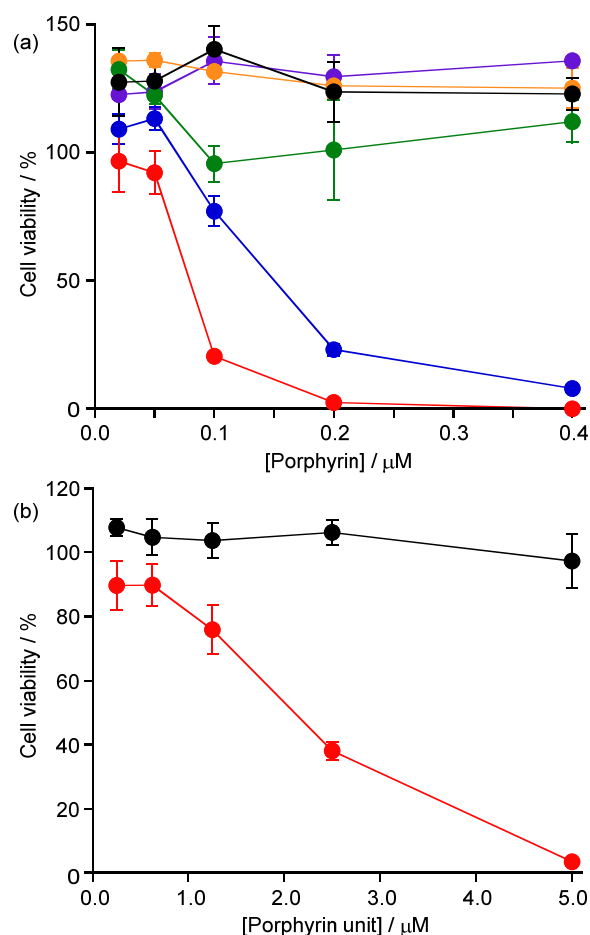


**Figure 4.** (a) Cell viability with the TMe- $\beta$ -CyD-complexed with **2** (purple line), **3** (orange line) and **4** (green line) in the dark and TMe- $\beta$ -CyD-complexed with **2** (blue line), **3** (red line) and **4** (black line) under photoirradiation (610–740 nm) for 30 min at different concentrations. (b) Cell viability with photofrin in the dark (black line) and under photoirradiation (red line) (610–740 nm) for 30 min at different concentrations. Cell viability was confirmed by the WST-8 method. Error bars represent the mean  $\pm$  standard deviation (SD) for  $n = 3$ .

The ROS in HeLa cells were identified through analyses of the inhibitory effect of L-histidine as a  $^1O_2$  scavenger and D-mannitol as a hydroxyl radical scavenger, respectively.<sup>21,22</sup> Figure 5 shows that the photocytotoxicity of the TMe- $\beta$ -CyD-complexed with **2** and **3** was effectively inhibited by L-histidine but was only weakly inhibited by D-mannitol. These results indicate that  $^1O_2$  played a major role in the photodynamic activity of the TMe- $\beta$ -CyD-complexed with **2** and **3** against HeLa cells.

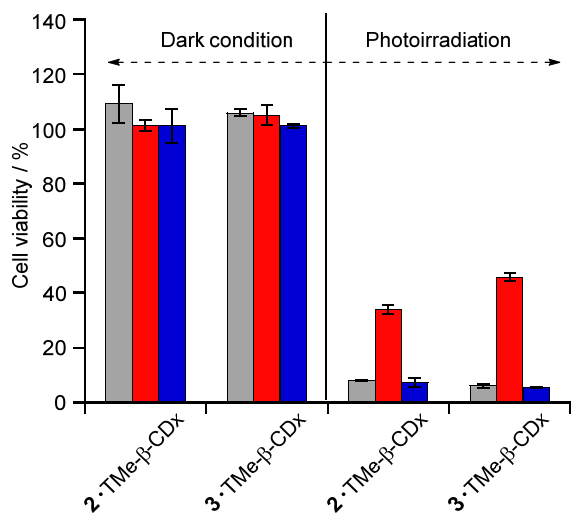


**Figure 5.** Inhibitory effect in the presence of ROS scavengers on the photodynamic activities of the TMe-β-CyD-complexed with **2** and **3**. The photodynamic activities of the TMe-β-CyD-complexed with **2** and **3** (0.8 μM) were measured in the absence (gray bar) and presence of 50 mM L-histidine (red bar) or 50 mM D-mannitol (blue bar). Error bars represent the mean ± standard deviation (SD) for  $n = 3$ .

The intracellular uptake by HeLa cells of the TMe-β-CyD complexed with **2–4** was observed with fluorescence microscopy at the emission wavelength of the porphyrin derivatives. As shown in Figure S6, all the TMe-β-CyD complexed with **2–4** possessed fluorescence peaks around 650 nm when they were excited at the wavelength ( $\lambda_{\text{ex}} = 540$  nm) used in the fluorescence microscopy. The fluorescence quantum yields were estimated to be 11.0% for **2**, 5.5% for **3**, and 9.2% for **4**. Although these values have some scatter, we judged that this would not affect the fluorescence microscopy results. The cells were incubated with the TMe-β-CyD-complexed with **2–4** at a concentration of 0.8 μM on a glass dish for 24 h in air with 5% CO<sub>2</sub> at 37 °C (Figure 6). Because fluorescences were observed by treatment with the TMe-β-CyD-complexed with **2** and **3**, neutral **2** and cationic **3** were taken up into HeLa cells (Figure 6b and 6d). Because the polar and hydrophilic groups of the compounds prohibit the transfer from the CyD cavities into the lipid membranes via an exchange reaction,<sup>12</sup> it is thought that compounds **2** and **3** released from the TMe-β-CyD cavities may not be directly incorporated into the plasma membranes of the HeLa cells. In contrast, anionic **4** was not taken up into HeLa cells (Figure 6f). To understand the mechanism of uptake of **2** and **3** by the cells, we investigated temperature dependence of uptake, as it is well-known that endocytosis can be inhibited at low temperatures.

After TMe-β-CyD-complexed **2** and **3** was added, HeLa cells were incubated for 30 min at 4 °C (Figure S7). The results clarified that the fluorescence of **2** and **3** (Figure S7d and S7h) was not observed, in contrast with that of the uptake at 37 °C (Figure S7b and S7f). This result indicated that **2** and **3** were taken up into the HeLa cells by endocytotic processes. Consequently, the result suggests that TMe-β-CyD-complexed with **2** and **3** did not decompose after uptake by HeLa cells. The results indicate that (i) intracellular

uptake of the neutral TMe-β-CyD-complexed with **2** increased due to interactions between the phenol moieties and the surface of the HeLa cells, (ii) uptake of the cationic TMe-β-CyD-complexed with **3** increased because of electrostatic interactions with the anionic cellular surface, while (iii) that of the neutral TMe-β-CyD-complexed with **2** decreased with the absence of phenolic hydroxy groups, and (iv) uptake of the anionic TMe-β-CyD-complexed with **4** decreased because of electrostatic repulsion. These results are consistent with those described in previous reports.<sup>23,24</sup> However, why was the neutral TMe-β-CyD-complexed with **2** taken up into HeLa cells? To investigate the effect of the phenol moiety, we used a TMe-β-CyD-complexed with **5**, with anisole moieties. Although the neutral TMe-β-CyD-complexed with **5** was also taken up into HeLa cells (Figure 6h), the fluorescence intensity was considerably weaker than that of the TMe-β-CyD-complexed with **2**. This result indicates that a hydroxy group in the phenol moieties of **2** is important for interaction with the surface of HeLa cells. Although the details are not yet clear, we suggest the existence of phenol receptors on HeLa cells. To show the existence of phenol receptors, we tried to evaluate the inhibitory effect using phenol. However, this led to cell death due to the high cytotoxicity of phenol.

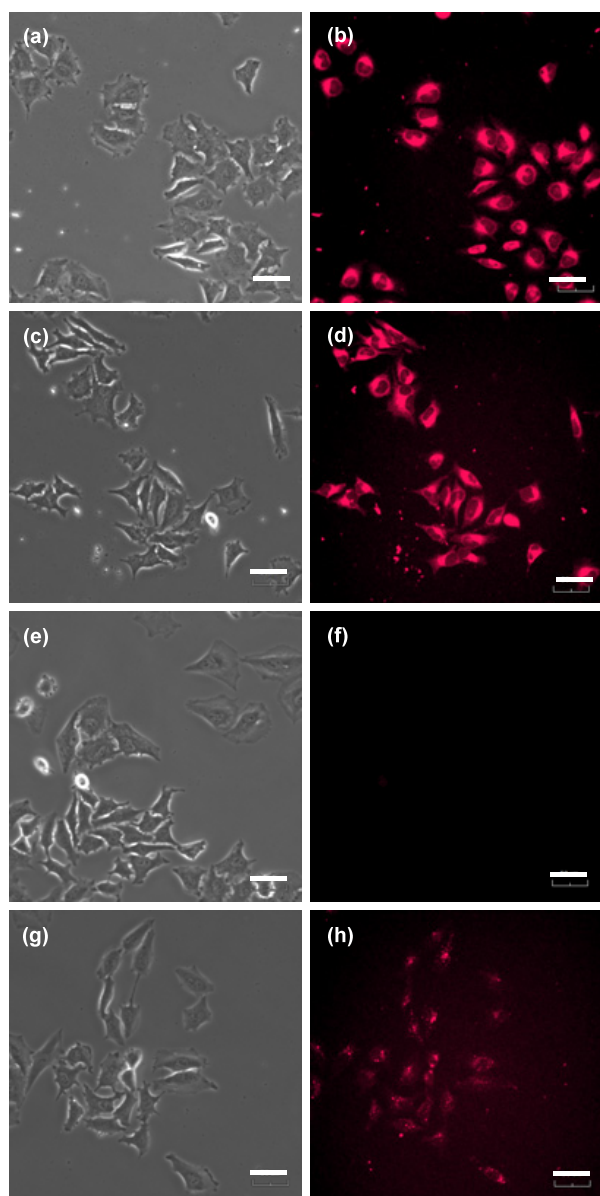


**Figure 6.** Phase contrast (a, c, e, and g) and fluorescence (b, d, f, and h) images of HeLa cells after being treated with (a and b) the TMe- $\beta$ -CyD-complexed with **2**, (c and d) the TMe- $\beta$ -CyD-complexed with **3**, (e and f) the TMe- $\beta$ -CyD-complexed with **4**, and (g and h) the TMe- $\beta$ -CyD-complexed with **5** for 24 h at 37 °C. The scale bar represents 50  $\mu$ m.

In summary, we have demonstrated that the photodynamic activity of TMe- $\beta$ -CyD-complexed with **2** and **3** was remarkably greater than that of TMe- $\beta$ -CyD-complexed with **4** toward HeLa cells under photoirradiation with wavelengths greater than 610 nm. The TMe- $\beta$ -CyD-complexed with **2** and **3** were approximately 14 and 26 times higher, respectively, in photodynamic activities than photofrin. The reasons for the high photodynamic activities of the TMe- $\beta$ -CyD-complexed with **2** and **3** can be attributed to high intracellular uptake into HeLa cells, rather than high  $^1\text{O}_2$  photoproduction abilities of the compounds. The fact that only a small amount of neutral TMe- $\beta$ -CyD-complexed with **5** were taken up into the HeLa cells suggests that the

phenol moieties in **2** are important for interaction with the surface of HeLa cells. Our findings therefore afford useful information to optimize the molecular design of TMe- $\beta$ -CyD-complexed with porphyrin derivatives as photosensitizers. Future research will include the development of TMe- $\beta$ -CyD-complexed with porphyrin derivatives with other substituents in *meso*-positions, for example hydroxy- and methoxy-substituted benzenes such as catechol, guaiacol, or 1,2-dimethoxybenzene.

## ASSOCIATED CONTENT

### Supporting Information

Supporting Information is available free of charge on the ACS Publications website.

Experimental procedures and UV-vis absorption and NMR spectra (PDF).

## AUTHOR INFORMATION

### Corresponding Author

\*E-mail: aikeda@hiroshima-u.ac.jp

### ORCID

Atsushi Ikeda: 0000-0003-3492-3455

### Author Contributions

The manuscript was written with contributions from all authors. All authors have given approval to the final version of the manuscript.

### Notes

The authors declare no competing financial interests.

## ACKNOWLEDGMENTS

This work was supported by JSPS KAKENHI Grant-in-Aid for Scientific Research (B) (Grant No. JP16H04133) and Grant-in-Aid for Challenging Exploratory Research (Grant No. JP16K13982) and the Electric Technology Research Foundation of Chugoku. We would like to thank Prof. J. Ohshita and Dr. Y. Adachi of Hiroshima University for the fluorescence measurements.

## ABBREVIATIONS

PS, photosensitizer; PDT, photodynamic therapy; ROS, reactive oxygen species; CyD, cyclodextrin; ABDA, 9,10-anthracenediyl-bis(methylene)dimalonic acid; NBT, nitroblue tetrazolium; IC<sub>50</sub>, half maximal inhibitory concentration.

## REFERENCES

- (1) Sternberg, E. D.; Dolphin, D. Porphyrin-based photosensitizers for use in photodynamic therapy. *Tetrahedron* **1998**, *54*, 4151–4202.
- (2) Chatterjee, D. K.; Fong, L. S.; Zhang, Y. Nanoparticles in photodynamic therapy: An emerging paradigm. *Adv. Drug Delivery Rev.* **2008**, *60*, 1627–1637.
- (3) Yano, S.; Hirohara, S.; Obata, M.; Hagiya, Y.; Ogura, S.; Ikeda, A.; Kataoka, H.; Tanaka, M.; Joh, T. Current states and future views in photodynamic therapy. *J. Photochem. Photobiol. C* **2011**, *12*, 46–67.
- (4) Henderson, B. W.; Dougherty, T. J. How does photodynamic therapy work? *Photochem. Photobiol.* **1992**, *55*, 145–157.

- (5) Bonnett, R.; White, R. D.; Winfield, U. J.; Berenbaum, M. C. Hydrophorophyrins of the meso-tetra(hydroxyphenyl)porphyrin series as tumour photosensitizers. *Biochem. J.* **1989**, *261*, 277–280.
- (6) Hirohara, S.; Obata, M.; Saito, A.; Ogata, S.; Ohtsuki, C.; Higashida, S.; Ogura, S.; Okura, I.; Sugai, Y.; Mikata, Y.; Tanihara, M.; Yano, S. Cellular uptake and photocytotoxicity of glycoconjugated porphyrins in HeLa cells. *Photochem. Photobiol.* **2004**, *80*, 301–308.
- (7) Hirohara, S.; Obata, M.; Alitomo, H.; Sharyo, K.; Ando, T.; Tanihara, M.; Yano, S. Synthesis, photophysical properties and sugar-dependent in vitro photocytotoxicity of pyrrolidine-fused chlorins bearing S-glycosides. *J. Photochem. Photobiol. B* **2009**, *97*, 22–33.
- (8) Ion, R. M.; Fierascu, R. C.; Neagu, M.; Constantin, C.; Stavaru, C. Porphyrin (TPP)-polyvinylpyrrolidone (PVP)-fullerene (C<sub>60</sub>) triad as novel sensitizer in photodynamic therapy. *Sci. Adv. Mater.* **2010**, *2*, 223–229.
- (9) Kano, K.; Tanaka, N.; Minamizono, H.; Kawakita, Y. Tetraarylporphyrins as probes for studying mechanism of inclusion-complex formation of cyclodextrins. Effect of microscopic environment on inclusion of ionic guests. *Chem. Lett.* **1996**, *25*, 925–926.
- (10) Kano, K.; Nishiyabu, R.; Asada, T.; Kuroda, Y. Static and dynamic behavior of 2:1 inclusion complexes of cyclodextrins and charged porphyrins in aqueous organic media. *J. Am. Chem. Soc.* **2002**, *124*, 9937–9944.
- (11) Kitagishi, H.; Chai, F.; Negi, S.; Sugiyurab, Y.; Kano, K. Supramolecular intracellular delivery of an anionic porphyrin by octaarginine-conjugated per-O-methyl- $\beta$ -cyclodextrin. *Chem. Commun.* **2015**, *51*, 2421–2424.
- (12) Ikeda, A.; Hino, S.; Mae, T.; Tsuchiya, Y.; Sugikawa, K.; Tsukamoto, M.; Yasuhara, K.; Shigeto, H.; Funabashi, H.; Kuroda, A. Porphyrin-uptake in liposomes and living cells using an exchange method with cyclodextrin. *RSC Adv.* **2015**, *5*, 105279–105287.
- (13) Tsuchiya, Y.; Shiraki, T.; Matsumoto, T.; Sugikawa, K.; Sada, K.; Yamano, A.; Shinkai, S. Supramolecular dye inclusion single crystals created from 2,3,6-trimethyl- $\beta$ -cyclodextrin and porphyrins. *Chem.–Eur. J.* **2012**, *18*, 456–465.
- (14) Tsuchiya, Y.; Yamano, A.; Shiraki, T.; Sada, K.; Shinkai, S. Single-crystal structure of porphyrin bicapped with trimethyl- $\beta$ -cyclodextrins: A novel dye-oriented material. *Chem. Lett.* **2011**, *40*, 99–101.
- (15) Berg, K.; Selbo, P. K.; Weyergang, A.; Dietze, A.; Prasmickaite, L.; Bonsted, A.; Engesaeter, B. O.; Angell-Petersen, E.; Warloe, T.; Frandsen, N., and Hogset, A. Porphyrin-related photosensitizers for cancer imaging and therapeutic applications. *J. Microsc.* **2005**, *218*, 133–147.
- (16) Lindig, B. A.; Rodgers, M. A. J.; Schaap, A. P. Determination of the lifetime of singlet oxygen in water-d<sub>2</sub> using 9,10-anthracene-dipropionic acid, a water-soluble probe. *J. Am. Chem. Soc.* **1980**, *102*, 5590–5593.
- (17) Doi, Y.; Ikeda, A.; Akiyama, M.; Nagano, M.; Shigematsu, T.; Ogawa, T.; Takeya, T.; Nagasaki, T. Intracellular uptake and photodynamic activity of water-soluble [60]- and [70]fullerenes incorporated in liposomes. *Chem.–Eur. J.* **2008**, *14*, 8892–8897.
- (18) Sugikawa, K.; Kubo, A.; Ikeda, A. pH-responsive nanogels containing fullerenes: synthesis via a fullerene exchange method and photoactivity. *Chem. Lett.* **2016**, *45*, 60–62.
- (19) Nakanishi, I.; Fukuzumi, S.; Konishi, T.; Ohkubo, K.; Fujitaka, M.; Ito, O.; Miyata, N. DNA Cleavage via superoxide anion-formed in photoinduced electron transfer from NADH to  $\gamma$ -cyclodextrin-bicapped C<sub>60</sub> in an oxygen-saturated aqueous solution. *J. Phys. Chem. B* **2002**, *106*, 2372–2380.
- (20) Bar, R.; Ulitzur, S. Bacterial toxicity of cyclodextrins: Luminous *Escherichia coli* as a model. *Appl. Microbiol. Biotechnol.* **1994**, *41*, 574–577.
- (21) Goldstein, S.; Czapski, G. Mannitol as an OH• scavenger in aqueous solutions and in biological systems. *Int. J. Radiol.* **1984**, *46*, 725–729.
- (22) Lindig, B. A.; Rodgers, M. A. J. Rate parameters for the quenching of singlet oxygen by water-soluble and lipid-soluble substrates in aqueous and micellar systems. *Photochem. Photobiol.* **1981**, *33*, 627–634.
- (23) Miller, C. R.; Bondurant, B.; McLean, S. D.; McGovern, K. A.; O'Brien, D. F. Liposome-cell interactions in vitro: Effect of liposome surface charge on the binding and endocytosis of conventional and sterically stabilized liposomes. *Biochemistry* **1998**, *37*, 12875–12883.
- (24) Ikeda, A.; Doi, Y.; Nishiguchi, K.; Kitamura, K.; Hashizume, M.; Kikuchi, J.; Yogo, K.; Ogawa, T.; Takeya, T. Induction of cell death by photodynamic therapy with water-soluble lipid-membrane-incorporated [60]fullerene. *Org. Biomol. Chem.* **2007**, *5*, 1158–1160.

---

Insert Table of Contents artwork here

